Anisotropic Flow of Identified Particles in Au + Au Collisions at $\sqrt{s_{NN}}$ = 3 - 3.9 GeV at RHIC

Zuowen Liu[1,*] for the STAR Collaboration

[1]Central China Normal University, Wuhan, Hubei 430079

Abstract. In these proceedings, we present transverse momentum dependence of the mid-rapidity slope of directed flow ($dv_1/dy|_{y=0}$) for π^+ and K_S^0 in Au + Au collisions at $\sqrt{s_{NN}}$ = 3.0, 3.2, 3.5, and 3.9 GeV. Both π^+ and K_S^0 show negative v_1 slope at low p_T (p_T < 0.6 GeV/c). Collision energy dependence of v_1 slope and p_T-integrated v_2 for $\pi^\pm$, K_S^0, and Λ are also presented. A comparison to JAM model calculations indicates that spectator shadowing can lead to anti-flow at low p_T. In addition, a breaking of the Number of Constitute Quark (NCQ) scaling of elliptic flow (v_2) is observed at $\sqrt{s_{NN}}$ = 3.2 GeV, which implies the dominance of hadronic degrees of freedom occurs in collisions at $\sqrt{s_{NN}}$ = 3.2 GeV and below.

1 Introduction

The goals of Beam Energy Scan (BES) program at Relativistic Heavy Ion Collider (RHIC) are searching for the possible QCD critical point and locating the first order phase boundary [1]. The energy dependence of net-proton v_1 slope [2] shows possible minimum at $\sqrt{s_{NN}} \approx$ 10 - 20 GeV, implies that the softest point of Equation of State (EoS) may exist within this range of collision energy. The existence of partonic collectivity is observed through NCQ scaling of v_2 at higher BES energies ($\sqrt{s_{NN}}$ > 7.7 GeV) [3], while the break NCQ scaling of v_2 at $\sqrt{s_{NN}}$ = 3.0 GeV [4] indicates the partonic collectivity is disappeared at this energy. In this contribution, we present the most recent measurements of directed flow (v_1) and elliptic flow (v_2) of identified particles ($\pi^\pm$, $K^\pm$, K_S^0, p, and Λ) at $\sqrt{s_{NN}}$ = 3.0 - 3.9 GeV in Fixed Target Au + Au collisions.

2 Experiment Setup

For identification of $\pi^\pm$, $K^\pm$, protons and anti-protons, a combination of Time Projection Chamber (TPC) [5] and Time of Flight (TOF) [6] is used. The left panel of Figure 1 illustrates the rigidity (p/q: particle momentum divided by charge) dependence of ionization energy loss (dE/dx) in the TPC. The dashed line represents the theoretical ionization energy loss curve for particle passing through the TPC. Particle identification by TOF is based on particle mass square (m^2) distribution, which can be obtained from particle velocity (β). Moreover, the Kalman Filter (KF) particle package [7], where the covariance matrix of reconstructed tracks is taken into account, is employed to reconstruct weak decay particles (K_S^0 and Λ). An example of reconstructing the invariant mass using the KF particle package is demonstrated with the K_S^0 meson in the right panel of Figure 1.

*e-mail: liuzw@mails.ccnu.edu.cn

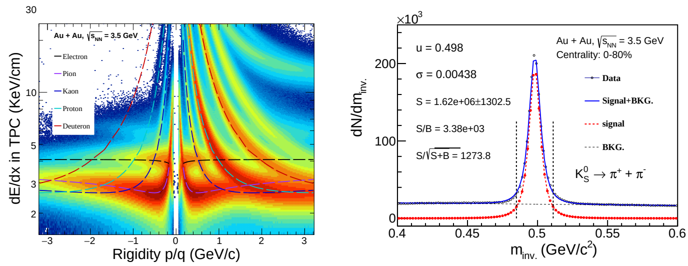

Figure 1. Left: Rigidity dependence of particle ionization energy loss in TPC. Right: Invariant mass distribution of K^0_S in Au + Au collisions at $\sqrt{s_{NN}}$ = 3.5 GeV.

3 Results

3.1 Anti-flow of Kaon

The anti-flow of kaon was first observed by E895 Collaboration at 6 A GeV [8]. It was attributed to the repulsive potential associated with the strange quark in K^0_S. We have observed anti-flow behavior in kaons and pions for $p_T < 0.6$ GeV/c in mid-central Au + Au collisions at $\sqrt{s_{NN}}$ = 3.0, 3.2, 3.5, and 3.9 GeV using the fixed target data from STAR. Figure 2 shows transverse momentum (p_T) dependence of v_1 slope ($dv_1/dy|_{y=0}$) for π^+ and K^0_S from STAR. The hadronic transport model JAM [9] calculations are compared with experimental data at 3.9 GeV. The JAM model in hadronic cascade mode (blue band) can successfully capture the anti-flow pattern at low p_T for π^+ and K^0_S, even without the inclusion of a kaon potential [8]. However, the JAM model with baryonic mean field (red band), tends to overestimate the v_1 slope for π^+ and K^0_S. Additionally, the JAM mean field without spectator contribution (black band) exhibits a larger v_1 slope compared to the one with spectators. The data-model comparisons suggest that the shadowing effect [10] from the spectator may also play a significant role in generating anti-flow at low p_T.

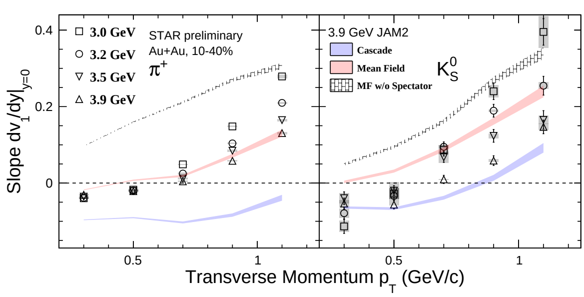

Figure 2. v_1 slope of π^+(left) and K^0_S(right) as function of transverse momentum and a comparison with JAM calculation at $\sqrt{s_{NN}}$ = 3.9 GeV.

3.2 NCQ Scaling of v_2

The left and right panels of Figure 3 illustrate the number of constituent quarks (n_q) scaled elliptic flow (v_2/n_q) as a function of transverse kinetic energy ($(m_T - m_0)/n_q$) for particles (π^+, K^+, K^0_S, p, and Λ) and the corresponding anti-particles (π^-, K^-, and K^0_S), respectively for Au + Au collisions at $\sqrt{s_{NN}}$ = 3.2 GeV. The NCQ scaling of v_2 is broken completely for particles and anti-particles at $\sqrt{s_{NN}}$ = 3.2 GeV. The existence of partonic collectivity is observed through NCQ scaling of v_2 at higher BES energies ($\sqrt{s_{NN}}$ > 7.7 GeV) [3]. The disappearing of NCQ scaling in v_2 at $\sqrt{s_{NN}}$ = 3.2 GeV implies that hadronic interactions play an important role at this energy and below [4, 11].

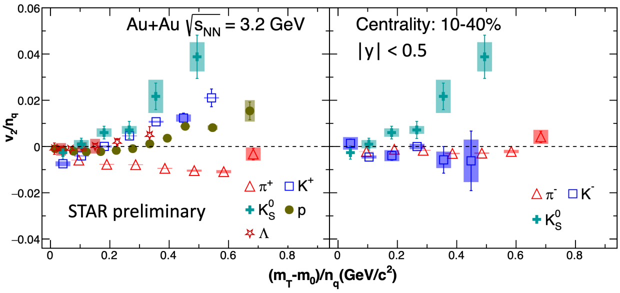

Figure 3. Number of Constituent Quark scaling of v_2 as a function of the scaled transverse kinetic energy for particles (left) and the corresponding anti-particles (right) at $\sqrt{s_{NN}}$ = 3.2 GeV.

3.3 Energy Dependence of v_1 and v_2

The top panel of Figure 4 shows collision energy dependence of v_1 slope in 10-40% mid-central Au + Au collisions at $\sqrt{s_{NN}}$ = 3.0 - 3.9 GeV. The v_1 slopes of π^+ (solid square) are negative at 3.0 - 3.9 GeV, while v_1 slopes of π^- (open square) are positive. The difference between π^+ and π^- may be explained by Coulomb effect [12]. Furthermore, v_1 slopes of K^0_S (solid triangle) are greater than π^+, v_1 slopes of Λ (solid circle) are largest among these four particle species. The v_1 slopes of all particles ($\pi^\pm$, K^0_S, and Λ) decrease in magnitude as collision energy increases. The lower panel in Figure 4 depicts the collision energy dependence of transverse momentum (p_T) integrated v_2. It is observed that the sign of v_2 changes from negative to positive for all particles ($\pi^\pm$, K^0_S, and Λ) within the collision energy range of $\sqrt{s_{NN}}$ = 3.0 - 3.9 GeV. This shift signifies the transition from out-of-plane to in-plane expansion [13], occurring specifically within the mentioned energy range.

The JAM calculations for Λ are represented by colored bands, with blue, red, and black bands corresponding to cascade, baryonic mean field, and mean field without spectators modes, respectively. The comparison of Λ v_1 between the data and model calculations suggests the presence of a strong baryon mean field [4] in the high baryon density region. Furthermore, the comparison between the measured p_T-integrated v_2 and model calculations indicates the significant influence of spectator shadowing in the energy range of $\sqrt{s_{NN}}$ = 3.0 - 3.9 GeV.

Summary

In summary, we present directed flow (v_1) and elliptic flow (v_2) measurements for identified particles ($\pi^\pm$, $K^\pm$, K^0_S, p, and Λ) in Au + Au collisions at $\sqrt{s_{NN}}$ = 3.0, 3.2, 3.5, and 3.9 GeV. The measurements for π^+ and K^0_S show negative v_1 slope ($dv_1/dy|_{y=0}$) at low p_T (p_T < 0.6 GeV/c). The transport model JAM reproduces anti-flow at low p_T without incorporating kaon potential, and indicates shadowing effect from spectator can lead to anti-flow. Secondly, NCQ scaling of v_2 is broken completely for particles (π^+, K^+, K^0_S, p, and Λ) and anti-particles (π^-, K^-) at $\sqrt{s_{NN}}$ = 3.2 GeV, implying that the hadronic interactions are dominant at $\sqrt{s_{NN}}$ = 3.2 GeV and below. At last, collision energy dependence of v_1 slope ($dv_1/dy|_{y=0}$) and p_T-integrated v_2 at $\sqrt{s_{NN}}$ = 3.0 - 3.9 GeV are presented. The v_1 slopes of all particles ($\pi^\pm$, K^0_S, and Λ) decrease in magnitude as collision energy increases. And the sign change in v_2 indicates that the change of out-of-plane to in-plane expansion happens between $\sqrt{s_{NN}}$ = 3.0 - 3.9 GeV.

Acknowledgement

This work was supported in part by the National Key Research and Development Program of China (Nos. 2022YFA1604900 and 2020YFE0202002); the National Natural Science Foun-

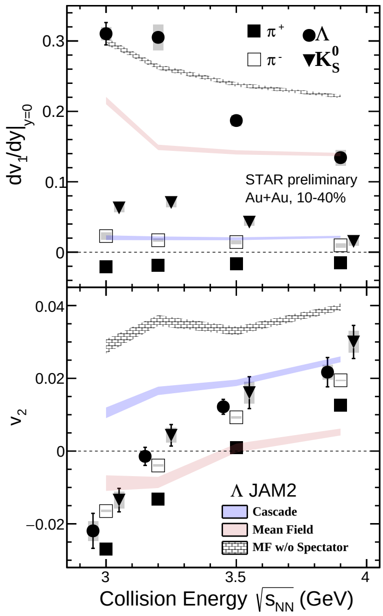

Figure 4. v_1 slope (top) and p_T-integrated v_2 (bottom) as a function of collision energy and compared with JAM calculation for Λ. Note that p_T windows for $\pi^{\pm}$, K^0_S, and Λ are $0.2 < p_T < 1.6$ GeV/c, $0.4 < p_T < 1.6$ GeV/c, and $0.4 < p_T < 2.0$ GeV/c, respectively. And the rapidity window is $-0.5 < y < 0$ for p_T-integrated v_2.

dation of China (Nos. 12175084); and Fundamental Research Funds for Central Universities (No. CCNU220N003).

References

[1] X. Luo, S. Shi, N. Xu, Y. Zhang, Particles **3**, 278 (2020)
[2] L. Adamczyk et al. (STAR Collaboration), Phys. Rev. Lett. **112**, 162301 (2014)
[3] L. Adamczyk et al. (STAR Collaboration), Phys. Rev. C **88**, 014902 (2013)
[4] M. Abdallah et al. (STAR Collaboration), Phys. Lett. B **827**, 137003 (2022)
[5] M. Anderson et al., Nucl. Instrum. Meth. A **499**, 659 (2003)
[6] W.J. Llope et al., Nucl. Instrum. Meth. B **241**, 306 (2005)
[7] A. Banerjee, I. Kisel, M. Zyzak, Int. J. Mod. Phys. A **35**, 2043003 (2020)
[8] P. Chung et al. (E895 Collaboration), Phys. Rev. Lett. **85**, 940 (2000)
[9] Y. Nara, A. Ohnishi, Phys. Rev. C **105**, 014911 (2022)
[10] H. Liu, S. Panitkin, N. Xu, Phys. Rev. C **59**, 348 (1999)
[11] S.W. Lan, S.S. Shi, Nucl. Sci. Tech. **33**, 21 (2022)
[12] U. Gürsoy, D. Kharzeev, E. Marcus, K. Rajagopal, C. Shen, Phys. Rev. C **98**, 055201 (2018)
[13] C. Pinkenburg et al. (E895 Collaboration), Phys. Rev. Lett. **83**, 1295 (1999)